NUMERICAL INVESTIGATION ON GAS-DISPLACEMENT OF VISCOPLASTIC MATERIALS IN CAPILLARY TUBES

Dione Alves de Sousa
Department of Mechanical Engineering, Universidade Federal do Espírito Santo, Avevida Fernando Ferrari. s/n, Goiabeiras, 29060-900, Vitória, ES, Brazil
dionesousa@petrobras.com.br

Edson José Soares
Department of Mechanical Engineering, Universidade Federal do Espírito Santo, Avevida Fernando Ferrari. s/n, Goiabeiras, 29060-900, Vitória, ES, Brazil
ejsoares2001@yahoo.com.br

Rogério Silveira de Queiroz
Department of Mechanical Engineering, Universidade Federal do Espírito Santo, Avevida Fernando Ferrari. s/n, Goiabeiras, 29060-900, Vitória, ES, Brazil
gradiva@terra.com.br>

Abstract. *The liquid displacement by gas injection occurs in many industrial processes like enhanced oil recovery, coating of internal surfaces of tubes and gas injection molding. Other important application is the mucus displacement process in pulmonary airways. These processes, characterized by presence of free surfaces, have been extensively studied both by theory and experiments in the case of Newtonian fluid. However, the complete understanding of the effects of the rheological properties of the displaced fluid in this type of flow is still under investigation. The goal of the present work is to analyze numerically the yield stress effect in this kind of processes.This was obtained by the solution of the complete two dimensional flow near the free surface, using the Galerkin Finite Element Method. The rheological character of the liquid was modeled by a simple Generalized Newtonian Model with the Papanastasiou function, to analyze the yield stress sensitivity of the displaced liquid. The main conclusion of the present work is that the fraction of the mass deposited on the tube wall decreases as the displaced fluid departs from Newtonian behavior. The predictions are confronted with numerical and experimental results available on the literature and a quite good agreement is obtained.*

Keywords*: Gas displacement, non-Newtonian liquids, viscoplastic materials, finite element method, free surface flows*

1. Introduction

The displacement of a liquid by a gas in internal passages occurs in many practical applications like mucus displacement in pulmonary airways, coating of catalytic converters and gas-assisted injection molding. As the gas pushes the liquid through the passage, a thin liquid layer is left attached to the wall. The thickness of this liquid film is an important parameter in many of these applications. For example, the fraction of mucus left behind gives the grade of obstruction of the airways; the correct coating thickness of a catalytic converter is essential; and, in gas-assisted injection molding, the thickness of the layer of material remaining on the wall determines the final strength of the hollow part being produced.

The flow of a gas pushing a Newtonian liquid in a capillary tube has been extensively studied both by theory and experiments. The goal was to understand the flow near the gas-liquid interface in order to determine the amount of liquid left on the tube wall as a function of the operating parameters and liquid properties. In many of the practical applications, however, the displaced liquid exhibits a non-Newtonian behavior, as is the case of polymer melts, polymeric solutions, pulmonary mucus and dispersions. The complete understanding of the effects of the rheological properties of the displaced liquid in this type of flow is still under investigation.

The thickness of the thin liquid layer attached to the wall is usually characterized in terms of the fractional deposited mass, m, or simply by the liquid film thickness left on the wall h_∞. The two forms are related by

$$m = \frac{mass\ left on\ the\ wall}{total\ mass} = 1 - \frac{displaced\ mass}{total\ mass} = \frac{V_b - \bar{u}}{V_b} = 1 - \left(\frac{D_b}{D_0}\right)^2 = 1 - \left(1 - \frac{2h_\infty}{D_0}\right)^2 \tag{1}$$

Where $h_\infty = (D_0 - D_b)/2$ is the layer thickness of the liquid left on the wall, D_0 is the tube diameter and D_b is the diameter of the cylindrical portion of the gas bubble, as illustrated in Fig. 1. The fractional mass can also be evaluated as a function of the bubble velocity V_b and the mean velocity of the liquid ahead of it, $\bar{u}$.

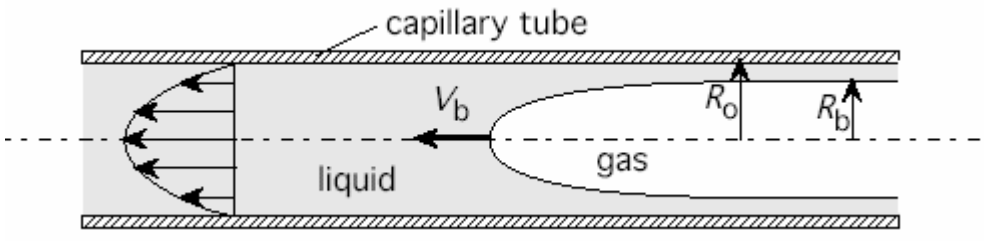

Figure 1. Gas-displacement of a liquid within a capillary tube

The first experimental analysis of gas-assisted displacement was done by Fairbrother and Stubbs (1935). They found an expression for m valid at small capillary numbers $Ca = \mu V_b / \sigma$ and Newtonian liquid:

$$m = \sqrt{Ca} \tag{2}$$

Taylor (1961) studied the same problem for a much larger range of capillary number. He found that the mass deposited on the tube wall asymptotically approaches *0.55* as *Ca* approaches *2*. He also suggested three possible streamline patterns of the liquid flow near the interface. At high capillary number, the flow would pass completely and no recirculation would appear near the free surface. The other two patterns would occur at intermediate to low capillary numbers, and they would be characterized by the position of the recirculation near the free surface. Cox (1962), continuing Taylor's study for a Newtonian viscous fluid, found experimentally that the amount of mass deposited on the tube wall asymptotically reaches *0.60* as the capillary number approaches *10.* He also predicted the shape of the interface using perturbation analysis. He concluded in his experiments that the flow is sensitive to the presence of the interface within a region about one and a half times the tube diameter long, situated ahead of the nose of the bubble. Furthermore, he concluded that the bubble reaches its final shape after it flows the same distance (one and a half times the tube diameter). In a second work, Cox (1964) investigated experimentally the streamline patterns suggested by Taylor and found a good agreement in the cases of high and low capillary number.

Bretherton (1961) investigated theoretically and experimentally the motion of long gas bubbles in tubes filled with Newtonian viscous liquid. He found a simple theoretical relationship for the mass deposited on the tube wall m, valid for low capillary number values, that agrees well with experimental measurements of Fairbrother and Stubbs (1935):

$$m = 2.68Ca^{2/3} \tag{3}$$

The penetration of a long gas bubble in a viscoelastic liquid was first studied experimentally by Huzyak and Koelling (1997). They were interested in identifying the influence of viscoelastic behavior on the fraction of mass deposited on the tube wall. The experiments were performed with a highly elastic liquid with a constant shear viscosity. The results were presented in terms of capillary number *Ca* and Deborah number *De*. They found that the fractional mass deposited on the wall begins to increase, relatively to Newtonian fluid, for De _ 1 and continues increasing over the entire range of *De* analyzed. Following the work of Huzyak and Koelling (1997), Gauri and Koelling (1999) analyzed the kinematics of the flow near the free surface using Particle Tracking Velocimetry (PTV).

The shear thinning behavior of the displaced liquid in this type of flow was studied by Poslinski and Coyle (1994). They used the Finite Element Method to solve the two-dimensional model of the flow. Kamisli and Ryan (1999) performed experiments and showed that the thickness of the deposited layer falls with the power-law index. They presented a singular perturbation analysis to model this situation, but their predictions followed the opposite trend of the experimental results. Soares, Carvalho and Souza Mendes (2005) also used the Finite Element Method to analyze the shear-thinning effect on gas-liquid displacement and the predictions followed the same trend observed experimentally. In addition, these authors investigated the influence of Reynolds number and viscoelastic effects, using an algebraic constitutive relation proposed by Thompson, Souza Mendes and Naccache (1999) to model the stress tensors.

Articles dealing with the analysis of gas-displacement of viscoplastic materials in capillary tubes are much scarcer. One of these few papers is given by Poslinsky, Oehler, and Stokes (1995) who reported experimentally the gas-assisted displacement of viscoplastic materials in tubes for two samples of viscoplastic materials. It can be concluded from their results that the fraction of mass attached on the wall falls as the yield-stress is increased. The yield-stress effect on gas-assisted displacement in tubes was also investigated by Dimakopoulos and Tsamopoulos (2003). They performed a numerical analysis by Finite Element Methods to solve the transient displacement of viscoplastic material by gas injection in straight and suddenly constrict tubes to investigate a number of operating parameters as Reynolds number and the pressure inlet beyond the yield-stress. The rheological character of the liquid was modeled by a simple Generalized Newtonian Model with the viscosity function proposed by Papanastasiou (1987). The effect of yield-stress

on the fractional mass deposited on the tube wall followed the same trend observed experimentally by Poslinsky, Oehler, and V.K. Stokes (1995) and by the predictions obtained in the present work, as will be showed later.

In this paper, the complete axissymmetric solution of the free-surface flow is obtained using the Galerkin Finite Element Method. The rheological behavior of the liquid is modeled by simple Generalized Newtonian Liquid model with the Papanastasiou´s viscosity function. The theoretical predictions for the fraction of mass deposited on the tube are compared with results from Dimakopoulos and Tsamopoulos (2003) and a quite good agreement is obtained.

2. Physical model

In this paper the flow near the gas-liquid interface is analyzed using a moving frame of reference attached to the tip of the bubble, as shown in Fig. 2. Relative to this reference frame the capillary tube wall moves with the interface velocity V_b while the interface is, of course, stationary.

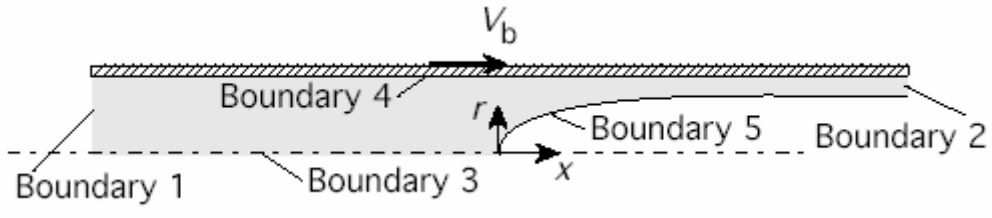

Figure 2. Flow domain for gas-displacement of liquid in a tube.

2.1. Conservation equations and boundary conditions

The flow near the interface is axissymmetric. The velocity and pressure fields, and the shape of the gas-liquid interface are governed by the continuity, Eq. 4, r-momentum, Eq. 5, and x-momentum, Eq. 6, equations, together with the appropriate boundary conditions.

$$\frac{1}{r}\frac{\partial}{\partial r}(rv)+\frac{\partial u}{\partial r}=0 \tag{4}$$

$$\rho\left(v\frac{\partial v}{\partial r}+u\frac{\partial v}{\partial x}\right)=\frac{1}{r}\frac{\partial}{\partial r}(rT_{rr})-\frac{T_{\theta\theta}}{r}+\frac{\partial T_{rx}}{\partial x} \tag{5}$$

$$\rho\left(v\frac{\partial u}{\partial r}+u\frac{\partial u}{\partial x}\right)=\frac{1}{r}\frac{\partial}{\partial r}(rT_{xr})+\frac{\partial T_{xx}}{\partial x} \tag{6}$$

In these equations, ρ is the mass density, and u and v are respectively the axial and radial components of the velocity field $\boldsymbol{u}$. The quantities T_{xx}, T_{xr}, T_{rx}, T_{rr} and $T_{\theta\theta}$ are the components of the stress tensor $\boldsymbol{T}$.

To facilitate the following description of the boundary conditions, the boundaries are labeled from 1 to 5, as illustrated in Fig. 2. Far enough upstream of the interface, Boundary 1, the flow is taken to be fully developed and the pressure is assumed to be uniform:

$$\boldsymbol{n}\cdot\nabla\boldsymbol{u}=0 \quad \text{and} \quad p=P_{in} \tag{7}$$

where $\boldsymbol{n}$ is the unit vector normal to the boundary surface and p is the pressure field.

Far enough downstream, Boundary 2, the traction vanishes:

$$\boldsymbol{n}\cdot\boldsymbol{T}=0 \tag{8}$$

Along the symmetry axis, Boundary 3, both the shear stress and the radial velocity vanish:

$$(\boldsymbol{n}\cdot\boldsymbol{T})\cdot\boldsymbol{t}=0 \quad \text{and} \quad \boldsymbol{n}\cdot\boldsymbol{u}=0 \tag{9}$$

Where $\boldsymbol{t}$ is a unit vector tangent to the boundary surface.

The no-slip and impermeability conditions are imposed along the tube wall, Boundary 4:

$$\boldsymbol{u}=V_b\boldsymbol{e}_x \tag{10}$$

Where $\boldsymbol{e}_x$ is the unit vector in the x-direction.

At the gas-liquid interface, Boundary 5, the traction balances the capillary pressure, and there is no mass flow across the interface:

$$\boldsymbol{n} \cdot \boldsymbol{T} = \left(\frac{\sigma}{R_m} - P_0 \right) \boldsymbol{n} \tag{11}$$

$$\boldsymbol{n} \cdot \boldsymbol{u} = 0 \tag{12}$$

In Eq. (11), σ is the liquid surface tension and $1/R_m$ is the local mean curvature of the interface, defined as:

$$\frac{1}{R_m} \boldsymbol{n} = \frac{1}{\sqrt{x_s^2 + r_s^2}} \frac{\partial \boldsymbol{t}}{\partial s} - \frac{x_s}{r\sqrt{x_s^2 + r_s^2}} \boldsymbol{n} \tag{13}$$

Where $\boldsymbol{t}$ is the unit tangent vector to the free surface, s is the arc-length curvilinear coordinate along the interface and $x_s = \partial x / \partial s$ and $r_s = \partial r / \partial s$ are spatial derivatives with respect to s.

2.2. Constitutive model

In order to close the set of differential equations, the stress tensor was related with the kinematics of the flow by the simple Generalized Newtonian Model. In this model, the stress tensor is given by:

$$\mathbf{T} = -p\mathbf{I} + \eta(\dot{\gamma})2\mathbf{D} \tag{14}$$

Where $2\boldsymbol{D} = \nabla \boldsymbol{u} + \nabla \boldsymbol{u}^T$ is the rate of strain tensor. The scalar quantity $\eta(\dot{\gamma})$ is the viscosity function, and $\dot{\gamma} \equiv \sqrt{2tr(\mathbf{D} \cdot \mathbf{D})}$ is the deformation rate. To analyze the effect of yield stress sensitive liquids, the viscosity function proposed by Papanastasiou (1987) was chosen, given by.

$$\eta = \mu + \frac{\tau_0 (1 - e^{-c\dot{\gamma}})}{\dot{\gamma}} \tag{15}$$

Where τ_0 is the yield stress, μ is an asymptotic viscosity value at high shear rate and c is a constant of adjustments. As suggested by a number of works presented on literature, c is chosen equal *1000*. For this value of the constant c, the Papanastasio´s viscosity function tends to the perfect plastic model, given by the Bingham viscosity function.

3. Numerical approach

Due to the free surface, the flow domain is unknown a priori. In order to solve this free-boundary problem by means of standard techniques for boundary value problems, the set of differential equations and boundary conditions written for the physical domain has to be transformed to an equivalent set, defined in a known reference domain. This subject is better discussed on papers of Kistler and Scriven (1983) and de Santos (1991). This transformation is made by a mapping $\boldsymbol{x} = \boldsymbol{x}(\boldsymbol{\xi})$ that connects the two domains, as shown in Fig. 3. A functional of weighted smoothness can be used successfully to construct the type of mapping involved here. The inverse of the mapping that minimizes the functional is governed by a pair of elliptic differential equations that are identical to those encountered in diffusional transport with variable diffusion coefficients. The coordinates ξ and η of the reference domain satisfy

$$\nabla \cdot (D_\xi \nabla \xi) = 0 \text{ and } \nabla \cdot (D\eta \nabla \eta) = 0 \tag{16}$$

where D_ξ and D_η are diffusion-like coefficients used to control the element spacing. Equations (16) describe the inverse mapping $\boldsymbol{\xi} = \boldsymbol{\xi}(\boldsymbol{x})$. To evaluate $\boldsymbol{x} = \boldsymbol{x}(\boldsymbol{\xi})$, the diffusion equations that describe the mapping also have to be transformed to the reference configuration. The gradient of the mapping $\boldsymbol{x} = \boldsymbol{x}(\boldsymbol{\xi})$ in a two dimensional domain is defined as $\nabla_\xi \boldsymbol{x} = \boldsymbol{J}$, and $\|J\| = det\, \boldsymbol{J}$ is the Jacobian of the transformation. Boundary conditions are needed in order to

solve the second-order partial differential equations (16). Spatial derivatives with respect to the coordinates of the physical domain $\boldsymbol{x}$ can be written in terms of the derivatives with respect to the coordinates of the reference domain ξ by using the inverse of the gradient of the mapping

$$\begin{pmatrix} \partial/\partial x \\ \partial/\partial y \end{pmatrix} = J^{-1} \begin{pmatrix} \partial/\partial \xi \\ \partial/\partial \eta \end{pmatrix} \tag{17}$$

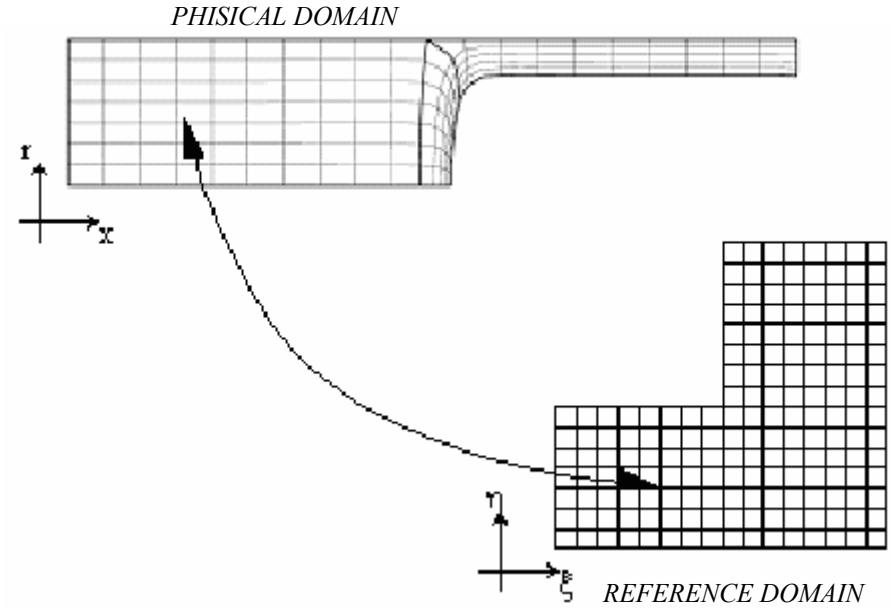

Figure 3. Mapping between the Physical and the reference domain

Along the solid walls and synthetic inlet and outlet planes, the boundary is located by imposing a relation between coordinates *x* and *y*, and stretching functions are used to distribute the nodal points of the finite element mesh along the boundaries. The free boundary (gas-liquid interface) is located by imposing the kinematic condition, Eq. (12). The discrete version of the mapping, Eq. (16), is generally referred to as mesh generation equations.

The differential equations that govern the problem and the mapping (mesh generation) equations were solved all together by the Galerkin/Finite Element Method. Biquadratic basis functions (ϕ_j) were used to represent the velocity and nodal coordinates, while linear discontinuous functions (χ_j) were employed to expand the pressure field. The velocity, pressure and node position are represented in terms of appropriate basis functions.

$$u = \sum U_j \phi_j \; ; v = \sum V_j \phi_j \; ; p = \sum P_j \chi_j \; ; x = \sum X_j \phi_j \; ; r = \sum R_j \phi_j \tag{18}$$

The coefficients of the expansions are the unknown of the problem:

$$C = \left[U_j \;\; V_j \;\; P_j \;\; X_j \;\; R_j \right]^T \tag{19}$$

The corresponding weighted residuals of the Galerkin method are:

$$R^i{}_{mx} = \int_{\bar{\Omega}} \left\{ \rho \phi_i \left(u \frac{\partial u}{\partial x} + v \frac{\partial u}{\partial r} \right) + \frac{\partial \phi_i}{\partial x} T_{xx} + \frac{\partial \phi_i}{\partial r} T_{xr} \right\} r \|\mathbf{J}\| d\bar{\Omega} - \int_{\bar{\Gamma}} \mathbf{e}_x \cdot (\mathbf{n} \cdot \mathbf{T}) \phi_i r \frac{d\Gamma}{d\bar{\Gamma}} d\bar{\Gamma} \tag{20}$$

$$R^i{}_{mr} = \int_{\bar{\Omega}} \left\{ \rho \phi_i \left(u \frac{\partial v}{\partial x} + v \frac{\partial v}{\partial r} \right) + \frac{\partial \phi_i}{\partial x} T_{xr} + \frac{\partial \phi_i}{\partial r} T_{rr} + \frac{\phi_i}{r} T_{\theta\theta} \right\} r \|\mathbf{J}\| d\bar{\Omega} - \int_{\bar{\Gamma}} \mathbf{e}_r \cdot (\mathbf{n} \cdot \mathbf{T}) \phi_i r \frac{d\Gamma}{d\bar{\Gamma}} d\bar{\Gamma} \tag{21}$$

$$R^i_{mx} = \int_{\bar{\Omega}} \rho \chi_i \left(\frac{\partial u}{\partial x} + \frac{1}{r}\frac{\partial}{\partial r}(rv) \right) r \|\mathbf{J}\| d\bar{\Omega} \tag{22}$$

$$R^i_x = -\int_{\bar{\Omega}} \left\{ D_\xi \nabla \xi \cdot \nabla \phi_i \right\} \|\mathbf{J}\| d\bar{\Omega} + \int_{\bar{\Gamma}} D_\xi (\mathbf{n} \cdot \nabla \xi) \phi_i \frac{d\Gamma}{d\bar{\Gamma}} d\bar{\Gamma} \tag{23}$$

$$R^i_r = -\int_{\bar{\Omega}} \left\{ D_\eta \nabla \eta \cdot \nabla \phi_i \right\} \|\mathbf{J}\| d\bar{\Omega} + \int_{\bar{\Gamma}} D_\eta (\mathbf{n} \cdot \nabla \eta) \phi_i \frac{d\Gamma}{d\bar{\Gamma}} d\bar{\Gamma} \tag{24}$$

Once all the variables are represented in terms of the basis functions, the system of partial differential equations reduces to simultaneous algebraic equations for the coefficients of the basis functions of all fields. This set of equations is non-linear and sparse. It was solved by Newton's method, and quadratic convergence was obtained as the residual approached zero. The linear system of equations at each Newton iteration was solved using a frontal solver. The domain was divided into 900 elements that correspond to 3801 nodes and 17904 degrees of freedom. A representative mesh is shown in Fig. 4.

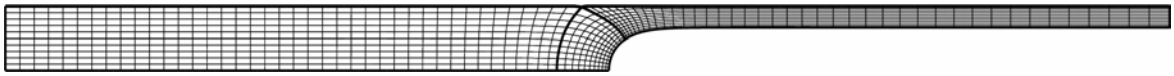

Figure 4. Representative Finite Element Mesh with 900 elements and 17904 unknowns

4. Results

The main goal of the present work is to analyze the flow near the interface for negligible Reynolds number as a function of the following dimensionless parameters defined by Eq. (25) and Eq. (26).

$$Ca = \frac{\eta_c V_b}{\sigma} = \frac{(\mu + \tau_0 / \dot{\gamma}_c) V_b}{\sigma} = \frac{[\mu + (\tau_0 R)/V_b] V_b}{\sigma} \tag{25}$$

$$\tau_0' = \frac{\tau_0}{\tau_c} = \frac{\tau_0}{\mu \dot{\gamma}_c + \tau_0} = \frac{\tau_0}{\mu (V_b / R) + \tau_0} \tag{26}$$

Where $\eta_c = \mu + (\tau_0 R)/V_b$ and $\tau_c = \mu (V_b / R) + \tau_0$ are respectively the characteristic viscosity and shear stress of the flow based on the characteristic deformation rate $\dot{\gamma}_c = V_b / R$.

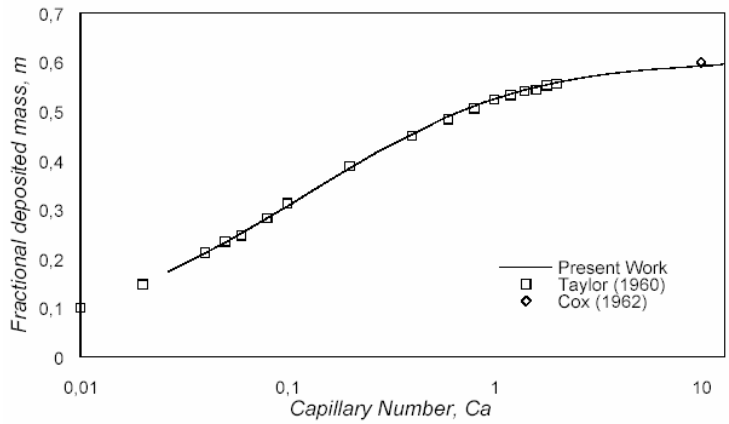

Figure 5. Fraction of mass deposited on the tube wall for a displaced Newtonian liquid

The predictions are focused in determining the amount of mass, Eq. (1), attached on the wall and the patterns of streamlines near the gas-liquid interface. In order to validate the theoretical model and the solution algorithm, the solution for the displacement of a Newtonian liquid was obtained. The predicted mass fraction, *m*, for a Newtonian liquid displaced by gas is shown in Fig. 5 together with the experimental results obtained by Taylor (1961) and Cox

(1962). It is seen that the agreement is quite good over the entire range of capillary number. Furthermore, on Table 1 is shown a comparison between the predictions obtained by the present work for viscoplastic liquids and results from the transient analysis of gas-displacement performed by Dimakopoulos and Tsamopoulos (2003). In this Table, m_∞ correspond to values of the fractional mass, m, obtained at high capillary numbers, when the fraction of mass asymptotically reaches a constant value over the entire range of yield stress analyzed.

Table 1. Comparison between the transient analysis of gas displacement from Dimakopoulos and Tsamopoulos (2003) and the present predictions.

τ_0'	m_∞ present work	m_∞ Dimakopoulos and Tsamopoulos (2003)
0.206	0.5857	0.5801
0.00891	0.5923	0.6006

In respect to a fixed reference frame, the dimensionless velocity profile as a function of dimensionless yield-stress τ_0' is showed on Fig. 6. Obviously, the plug flow region increases as the liquid behavior departure from Newtonian case, i.e., as τ_0' is incremented over the range $0 \le \tau_0' \le 0.85$.

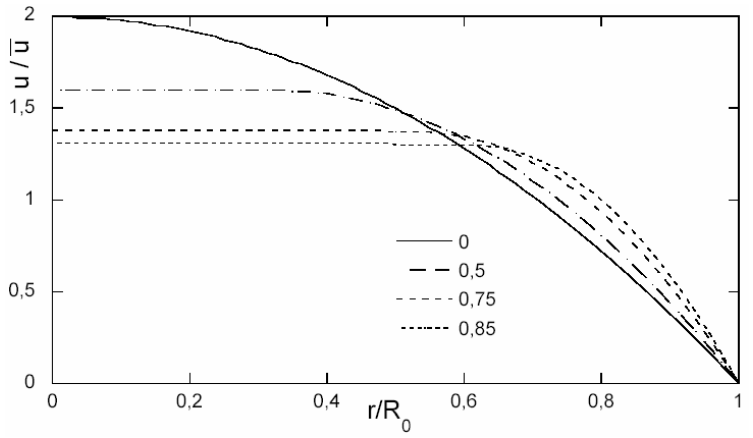

Figure 6. Dimensionless velocity profile in the fully developed flow in a region sufficiently distant from the tip of the interface as a function of τ_0' .

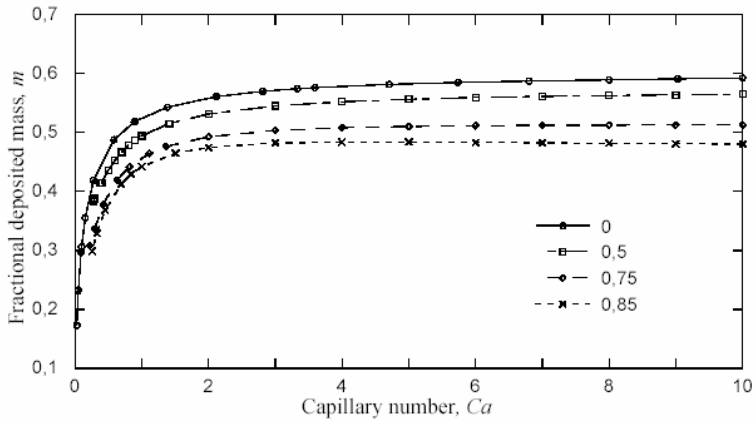

Figure 7. Fraction of mass deposited on the wall as a function of capillary number for $\tau_0' = 0\,;0.5\,;0.75\,;0.85$

The effect of the dimensionless yield stress, τ_0' , on the fraction of mass, m, deposited on the wall is showed at Fig. 7. Over the entire range of capillary number studied, the predictions suggest that the liquid film attached on the wall falls as the material departure from Newtonian behavior, i.e., as τ_0' increase. These predictions are in agreement with

theoretical study performed by Dimakopoulos and Tsamopoulos (2003) and experimental results obtained by Poslinsky, Oehler, and Stokes (1995). In addiction, over the range of τ_0' studied, it can be conclude that *m* tends to an asymptotic value as the capillary number, *Ca*, is incremented. This asymptotic value is reached faster as the liquid departure from Newtonian case.

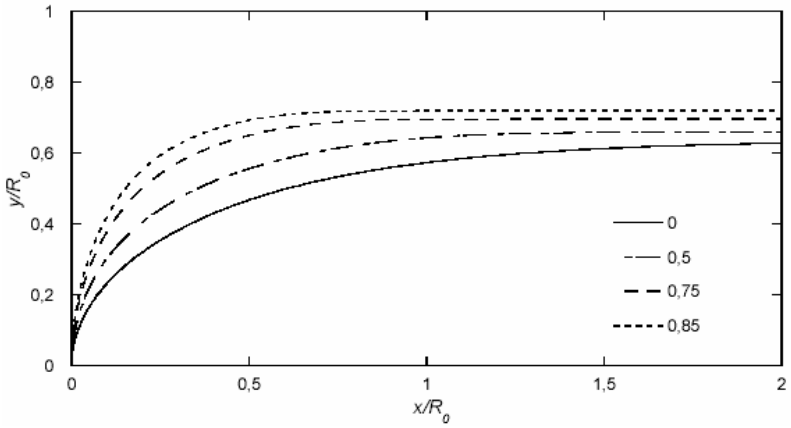

Figure 8. Free surface profile at *Ca=10* and $\tau_0' = 0\,;0.5\,;0.75\,;0.85$

Figure 8 shows the shape of the tip of the free surface at high capillary number, *Ca=10*, as a function of dimensionless yield-stress number, τ_0'. The tip of the interface tends to be flatter as the liquid departure from Newtonian behavior and, consequently, a quite larger uniform radius belong the interface is obtained when viscoplastic liquids are displaced by gas. For example, the cylindrical form of the free surface for the liquid with $\tau_0' = 0.85$ is observed in $0.75R_0$ from of the tip of the interface while for Newtonian case, $\tau_0' = 0.$, the cylindrical portion start only in $2R_0$ from the free surface front.

5. Final remarks

A two-dimensional model of the flow near the interface of a gas displacing a viscoplastic liquid in a capillary tube was analyzed. The presence of the free surface makes the solution of the problem rather complex; the domain where the governing differential equations are integrated is unknown a priori. A fully coupled formulation was used and the differential equations were solved by the Galerkin Finite Element Method. The simple constitutive model of Generalized Newtonian Liquid with a viscosity function proposed by Papanastasiou (1987) was used to relate the stress tensor with the kinematics of the flow.

The predictions of the fractional deposited mass, *m*, for the gas-displacement of Newtonian liquid were compared with experimental data reported from Taylor (1961) and Cox (1962) and a quite good agreement was attained. In addiction, the numerical analysis of the transient displacement of a viscoplastic liquids performed by Dimakopoulos and Tsamopoulos (2003) was also confronted with the present work and, again, a satisfactory agreement was observed.

The study of yield stress sensitivity indicates that the liquid film attached on the tube wall falls and the shape of the free surface becomes flatter as the liquid departs from Newtonian behavior.

6. References

Bretherton, F. P., 1961, "The Motion of Long Bubbles in Tubes," Journal of Fluid Mechanics, Vol. 10, pp. 166–188.

Cox, B. G., 1962, "On Driving a Viscous Fluid Out of a Tube," Journal of Fluid Mechanics, Vol. 14, pp. 81–96.

Cox, B. G., 1964, "An experimental investigation of the streamlines in viscous fluid expelled from a tube", Journal of Fluid Mechanics Vol. 20, pp. 193–200.

Dimakopoulos, Y. and Tsamopoulos, J., 2003, " Transient Displacement of a Viscoplastic Material by Air in Straight and Constricted tubes", Journal of Non-Newtonian Fluid Mechanics, Vol. 112, pp. 43-75.

Fairbrother, F., and Stubbs, A. E.,1935, "Studies in Electroendosmosis. Part VI. The Bubble-Tube Methods of Measurement," J. Chem. Soc., Vol. 1, pp. 527–529.

Gauri, V., Koelling, K. W., 1999. "Gas-assisted displacement of viscoelastic fluids: Flow dynamics at the bubble front," J. Non-Newt. Fluid Mech, Vol. 83, pp. 183–203.

Huzyak, P. C., Koelling, K. W., 1997, "The penetration of a long bubble through a viscoelastic fluid in a tube," Journal of Non-Newtonian Fluid Mechanics, Vol. 71, pp. 73–88.

Kamisli, F., Ryan, M. E., 1999, "Perturbation method in gas-assisted power law fluid displacement in a circular tube and retangular channel," Chem. Eng. J., Vol. 75, pp. 167–176.

Papanastasiou, T., C., 1987, "Flows of Materials with Yield-Stress", Journal of Rheology, Vol.31 pp. 385-404.

Poslinski, A. J., Coyle, D. J., 1994, "Steady gas penetration through non-Newtonian liquids in tube and slit geometries: Isothermal shear thinning effects, "Proceedings of Polymer Processing Society Annual Meeting, pp. 219–219.

Poslinski, A. J., Oehler, P., O. and Stokes, V., K., 1995, "Isothermal gas-assisted displacement of a viscoplastic liquid in tubes", Polimer Engineering and Science, Vol. 35, pp. 877-892.

Soares, E. J., Carvalho, M. S., Souza Mendes, P. R., 2005, "Immiscible liquid-liquid displacement in capillary tubes," Journal of Fluids Engineering, Vol. 127 (1), pp. 24-31.

Taylor, G. I., 1961, "Deposition of a Viscous Fluid on the Wall of a Tube", Journal of Fluid Mechanics, Vol. 10, pp. 161–165.

Thompson, R. L., Souza Mendes, P. R., Naccache, M. F., 1999, "A new constitutive equation and its performance in contraction flows", Journal of Non-Newtonian Fluid Mechanics, Vol. 86, pp. 375–388.

7. Responsibility notice

The authors are the only responsible for the printed material included in this paper.